Journal of Advanced Zoology

ISSN: 0253-7214
*Volume **44** Issue **S-6 Year 2023** Page **1453:1462***

Synthesis of Composite Corrosion Inhibitor Based on Maleic Anhydride, Monoethanolamine and Phosphate Acid

Choriev I.K.[1*], Turaev Kh. Kh.[2], Babamuratov B. E.[3], Durdibayeva R. M.[4], Muzaffarova N. Sh[5]

[1]Faculty of Chemistry, Termez State University, st. Barkamol avlod, 43, Termez, Uzbekistan, 190111
Email: choriyevi@tersu.uz ORCID -0009-0005-3437-7564
[2]Faculty of Chemistry, Termez State University, st. Barkamol avlod, 43, Termez, Uzbekistan, 190111
Email: hhturaev@rambler.ru ORCID -0000-0002-0627-5449
[3]Associate Professor, Dean of Medical Faculty, Termiz University of Economics and Service. Termiz, Uzbekistan,190111. Email: babamuratov1985@mail.ru
[4]Department of oil and gas technology, Karakalpak State University,
Gmail: durdubaevaroza@gmail.com
[5]Head of the Department of Medical and Biological Chemistry, Termiz branch of the Tashkent Medical Academy
Gmail: hilolanazokat2010@gmail.com. ORCID: (0000-0002-9419-2300).

**Corresponding author's E-mail: choriyevi@tersu.uz*

Article History

Received: 06 June 2023
Revised: 05 Sept 2023
Accepted: 06 Dec 2023

Abstract

In this article, the optimum conditions for the synthesis of corrosion inhibitors based on maleic anhydride, monoethanolamine, and phosphoric acid and the inhibitory efficiency of the obtained inhibitor are studied. In this case, the mole ratio of the starting materials was 2 moles (122 g) of monoethanolamine: 1 mole (98 g) of maleic anhydride: 1 mole (98 g) of phosphoric acid, and the yield of the reaction was 92.5%. The IR spectra of the structure of this obtained inhibitor were studied. The inhibition efficiency of this corrosion inhibitor was measured by the gravimetric method according to GOST 9.506-87 in 1M HCl + 200 mg/l NaCl and 0.5 HCl + 200 mg/l NaCl environments. The inhibition efficiency was 93.15% and 92.86%, respectively. reached According to the results of the electrochemical research, the inhibition efficiency was 91.5%. In addition, Langmuir, Frumkin, and Tyomkin isotherms of the inhibition mechanism of the inhibitor were studied. The effect of the inhibitor on the steel surface was studied with a scanning electron microscope.

Keywords: *Materials, Microscope*

1. Introduction

Corrosion is a reversible process, which converts pure metal to different chemical compounds [1]. Nowadays, corrosion is turning into a major issue in many industries, building materials, infrastructure, tools, ships, trains, vehicles, machines, and appliances [2]. Carbon steel experiences extensive corrosion during the cleansing process with acids. The NACE 2016 reported shows that at the world level about 2.5 trillion U.S. dollars economic fall caused by corrosion every year total of 10% of total metal of world is lost due to corrosion which influences the economy of the nation [3]. Corrosion is not only responsible for an economic loss but also associated with safety issues because it decreases the shelf life of steel [4]. This problem turns into a major issue for the entire world, so researchers are trying to address this issue in various ways [5]. An inhibitor is a substance which when added to an environment in small concentration [6]. In the following studies, corrosion inhibitors were obtained based on methyl methacrylate, poly (methyl methacrylate-maleic anhydride) P(MMA-MAH) with different percentages methyl methacrylate and maleic anhydride were synthesized and the inhibitory potential of this inihitor on simple carbon steel in a 0.5 M HCl environment studied [7,8]. A new *N*-heterocyclic initiator *N*-[2-(8-heptadecenyl)-4,5-dihydro-1*H*-imidazole-1-ethyl]-2-bromoisobutyramide was synthesized [9,10].

2. Materials And Methods

Materials. To synthesize this composite corrosion inhibitor, monoethanolamine and methyl methacrylate monomers (purified by driving in inert nitrogen atmosphere) and phosphoric acid, such as 1M HCl + 200 mg/l NaCl for aggressive environments, were used. Steel composition: Fe 97.755-97.215%, C 0.17-0.24%, Si 0.17-0.37, Mn 0.35-0.65%, Ni 0.3%, S 0.04 %, P 0.035 %, Cr 0.25 %, Cu 0.3 %, As 0.08 %. 2×2.5 cm^2 samples of steel with this composition were taken, the surface was cleaned with sandpapers, washed several times in acetone and dried.

Methods. The obtained research results were analyzed by Infrared Spectroscopy (IR) - IR Spectra of Synthesized Corrosion Inhibitors "IRTracer-100" (SHIMADZU CORP., Japan, 2017) Spectrometer, Scanning Electron Microscope (SEM, SmartSEM software SEM-EVO MA 10 (Carl Zeiss, Germany),). electrochemical studies were studied using devices such as the CS-350 Cossion test.

Experimental part

Synthesis of composite corrosion inhibitor. This reaction is the reverse of the above process, that is, the process proceeds with the release of a large amount of heat. It is explained that one of the main reasons for this is not only the high reaction activity due to the presence of two functional groups in the composition. Based on this property, a 500 ml flask with a flat bottom is taken, first, 2 moles (122 g) of monoethanolamine are poured into it and the system is cooled in the presence of cooling agents (mainly chilled water). While stirring the reaction mass, 1 mole (98) of maleic anhydride is slowly added to the reaction mixture. The mixture was stirred for 45 minutes and the intermediate product was obtained with a yield of 92.5%. 1 mol (98 g) of phosphoric acid is slowly added dropwise to the intermediate product obtained based on monoethanolamine and maleic anhydride and mixed (Fig. 2.1). The resulting intermediate product has the following physicochemical properties:

Table-2.1. Physico-chemical properties of MMF-1 brand corrosion inhibitor

№	Aggregate status	pH	Density g/cm2	Solvent
MMF-2	An interesting colored, dark substance	5,4	1,37	In hot water

IR-spectrium analyses. The obtained reaction product was analyzed by IR-spectra methods.

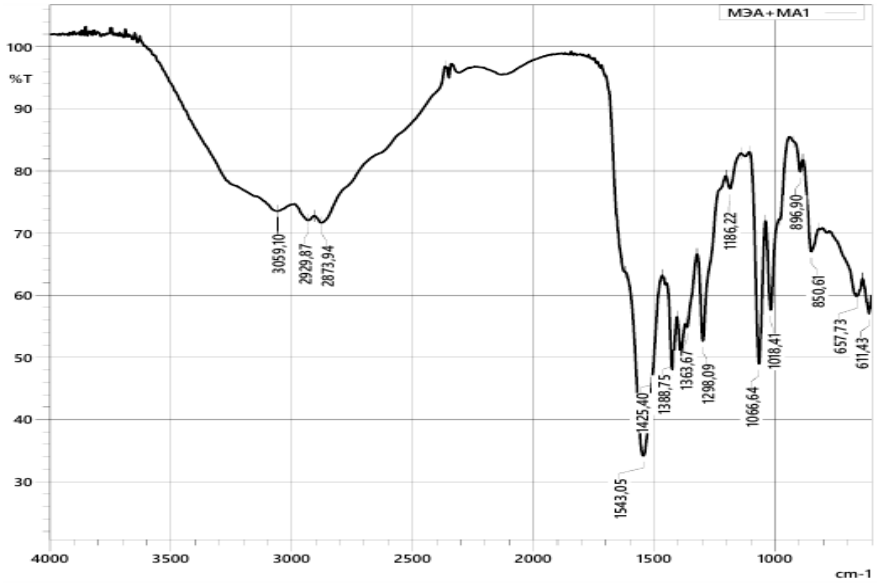

Figure 2.1. IR-spectra of MMF-1 composite corrosion inhibitor.

From the IR spectrum analysis of the intermediate product of MMF-2 corrosion inhibitor, we can see that the valence vibrations of the OH group were observed in the broad and intense absorption region of 3059.10cm^{-1}. Valence vibrations of -C-N- bonds to the area of 1298.09-1182.62 cm^{-1}, asymmetric valence vibrations of -C-O-C- bonds in the area of 1298.09 cm^{-1}, valence, intensive vibration frequencies of -C-OH groups 1186.22 cm^{-1} Valence and intensity fluctuations were observed in the range of -1 field.

3. Results and Discussion

TABLE 1. Study of determination of inhibition and protection levels of corrosion inhibitors using gravimetric method. Determination of inhibition efficiency of composite corrosion inhibitor by gravimetric method was carried out by GOST 9.506-87. In this case, the temperature was between 30 ^{0}C and 80 ^{0}C, and the speed of the moving liquid was 1.1 m/s.

The inhibition efficiency of the obtained composite corrosion inhibitor was studied at concentrations of 75, 100, 150, and 200 mg/l, and the optimal concentration here was 200 mg/l. Based on the research results, the optimum inhibitory concentration of corrosion inhibitors was assumed to be 200 mg/l concentration [11,12].

Table-3.1. Turli harorat va kontsentratsiyada MMF-1 markali ingibitorining Fon-1dagi korroziyaga qarshi turish.

Inhibitor	**T,** (K)	**C,** (mg/l)	***W,*** gr/(sm^2·hour)	**γ**	**η,** (%)	**θ**
MMF-1	**303**	-	**1,24**	-	-	-
		75	0,298	4,18	76,45	0,7645
		100	0,234	5,32	81,23	0,8123
		150	0,144	8,49	88,27	0,8827
		200	0,105	11,92	91,89	0,9189
	313	-	1,53	-	-	-
		75	0,353	4,29	76,72	0,7672
		100	0,263	5,76	82,62	0,8262
		150	0,16	9,44	89,4	0,894
		200	0,112	13,45	92,56	0,9256
	323	-	1,74	-	-	-
		75	0,397	4,4	77,27	0,7727
		100	0,291	5,99	83,32	0,8332
		150	0,178	9,78	89,78	0,8978
		200	0,123	14,11	92,92	0,9292
	333	-	1,89		-	-
		75	0,432	4,43	77,44	0,7744
		100	0,317	6,04	83,47	0,8347
		150	0,195	9,85	89,85	0,8985
		200	0,133	14,58	93,15	0,9315

From Table 3.1, we can see that 60 0C is 93.15% in a strong aggressive environment such as 1M HCl + 200 mg/l NaCl at a concentration of 200 mg/l.

Table-3.2. Corrosion effectiveness of MMF-1 brand inhibitor in Fon-2 solution at different temperatures and concentrations

Inhibitor	**T,** (K)	**C,** (mg/l)	***W,*** gr/(sm^2·hour)	**γ**	**η,** (%)	**θ**
MMF-1	**303**	-	**1,24**	-	-	-
		75	0,287	4,39	77,15	0,7715
		100	0,226	5,57	82,02	0,8202
		150	0,137	9,19	89,13	0,89,13
		200	0,101	12,47	92,01	0,9201
	313	-	**1,53**	-	-	-
		75	0,336	4,55	78,01	0,7801
		100	0,253	6,05	83,43	0,8343
		150	0,17	9	88,41	0,8841
		200	0,107	14,29	92,97	0,9297
	323	-	**1,77**	-	-	-
		75	0,373	4,74	78,89	0,7889
		100	0,272	6,38	84,61	0,8461
		150	0,185	9,56	89,57	0,8957
		200	0,121	14,62	93,11	0,9311
	333	-	**1,93**		-	-
		75	0,402	4,8	79,13	0,7913
		100	0,285	6,77	85,22	0,8522
		150	0,191	10,1	92,32	0,9232

		200	0,128	14,07	92,86	0,9286

It is known from Table 3.2 that 0.5 HCl+200 mg/l NaCl was 92.86% at 333 K due to high absorption on the metal surface with increasing temperature[13]..

Electrochemical studies. One of the most reliable methods for determining the inhibition efficiency of corrosion inhibitors is the electrochemical method. As a result of the absorption of inhibitors on the surface of the steel electrode, there is a change in the potential difference and the amount of corrosion current in the electrodes. The process of polarization occurs because the potentials at the cathode and anode do not have a constant value.

Electrochemical studies of these MMF-2 brand corrosion inhibitors were studied in Fon-1 corrosion environments at a temperature of 20 ^{0}C. Inhibition efficiency of Fon-1(1M HCl+200 mg/l NaCl) without inhibitor at different (50, 100, 150 and 200) concentrations of St2 steel o studied.

In general, when the Tafel curves are studied in the medium with and without the inhibitor, the amount of corrosion current is higher in the medium without the inhibitor, which increases the formation of hydrogen and chloride ions in the solution and stimulates the acceleration of the dissolution of the cathode and anode. However, in environments where corrosion inhibitors are added to the corrosive environment, the Tafel curves show that the amount of corrosion current decreases, that is, the corrosion inhibitors reduce the melting of steel to a maximum level due to the slowing down of the cathode and anode dissolution. It is known from the results of the research that the concentration of the inhibitor depends on the change of the Tafel curves, which shows how much of the inhibitor molecules cover the steel surface [15].

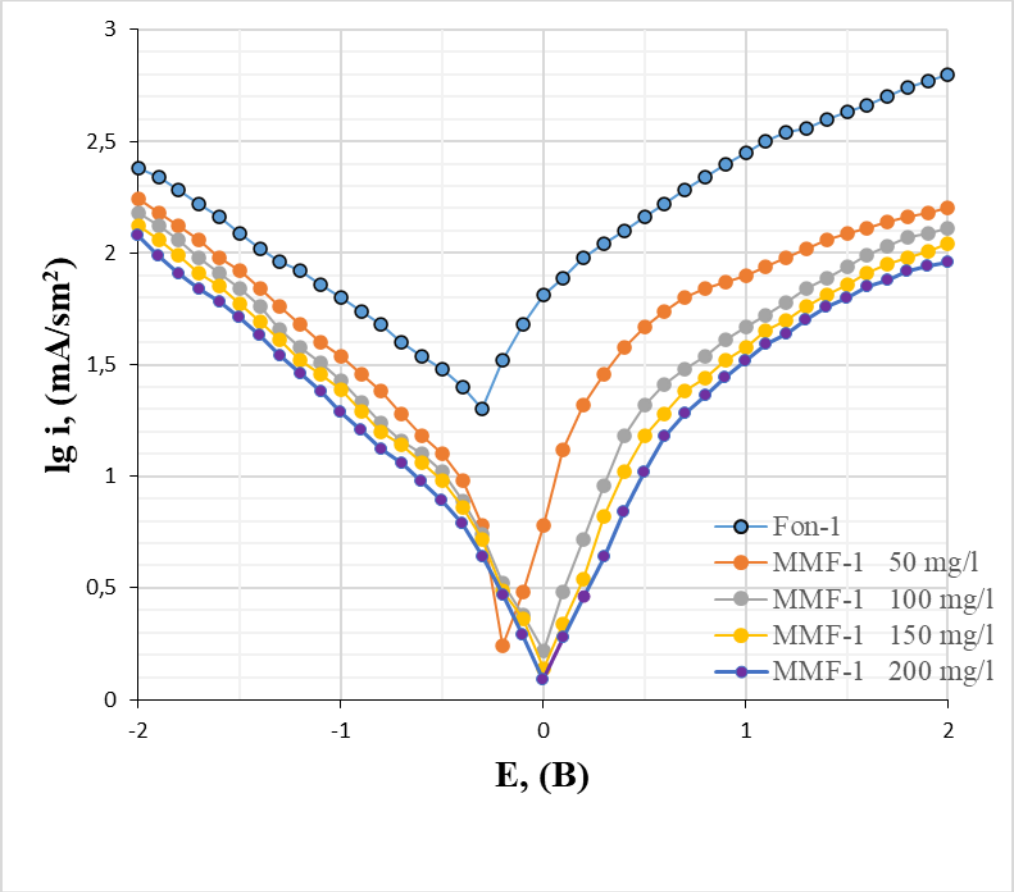

Figure 3.1. Polarization curves of the steel electrode in the Fon-1 solution in the presence of solutions without and with inhibitors.

Tafel curves (Fig. 3.12) of corrosion current density (i_{corr}), corrosion rate (CR_{PDP}), corrosion potential (E_{corr}), β_a and $\beta_c$slopes were obtained (Table 3.3).

Table-3.3. The efficacy of the inhibitor is determined by the method of polarization curves in solution with inhibitor (MMF-1) and without inhibitor.

Inhibitor	**C,** (mg/l)	***i,*** (mA/cm^2)	**γ**	**θ**	**η,** (%)
Fon-1	-	56,1	–	–	–
MMF-1	50	8,63	5,06	0,821	82,1

	100	6,22	5,83	0,837	83,7
	150	4,13	7,24	0,861	86,1
	200	2,21	11,81	0,915	91,5

From Table 3.3, we can see that the amount of corrosion current is high (56.1 mA/cm2) in solutions without inhibitor, but the amount of corrosion current decreases accordingly with the introduction of an inhibitor into the system and the increase of the concentration of the inhibitor. For example: 8.63 mA/cm^2 at 50 mg/l, 6.22 mA/cm^2 at 100 mg/l, 4.13 8.63 mA/cm^2 at 150 mg/l and 2.21 at 200 mg/l reduced to mA/cm^2.

Due to the formation of a complex with Fe^{2+} ions, this MMF-1 brand corrosion inhibitor blocks cathodic reactions, reduces the release of hydrogen and prevents anode and cathode melting. Inhibition efficiency was 91.5% at 200 mg/l[16]..

When smaller concentrations of the inhibitor are effectively adsorbed on the metal surface in a straight direction, its inhibition efficiency can be even higher. In conclusion, it can be said that the adsorption mechanism depends on the concentration, and with the increase in the concentration, the electrostatic repulsion and the forces between the inhibitor molecules increase with the increase of the concentration, which leads to the adsorption mechanism of a straight direction along the metal surface.

Thermodynamic and kinetic. By finding the activation energy of the obtained composite corrosion inhibitors at different concentrations and temperatures, it is possible to study the mechanism of interaction of the inhibitors with the metal surface. The corrosion rate is determined using the Arrhenius formula to determine the activation energy in solutions with and without inhibitors.

$$CR=A\exp(\frac{-\mathrm{Ea}}{\mathrm{RT}}) \qquad (3.1)$$

Here: Ea is the activation energy expressed in kJ/mol moles, R is the universal gas constant value of 8.314 J/mol×K, and T is the temperature expressed in K A-exponential coefficient.

If we compare the activation energy (E_a) of the solutions with an inhibitor to the solution without the inhibitor, we can see that (E_a) increases as a result of the addition of the inhibitor to the solution, and the activation energy also increases with the increase in the concentration of the inhibitor in the solution. A high activation energy causes physical adsorption, and if it does not change or becomes less, it causes chemical adsorption.

As the inhibitor concentration increased, the activation energy (Ea) values also increased dramatically. Therefore, in preventing corrosion, the primary function of the inhibitor is physical adsorption on the metal surface. From the large negative values of entropies, we can see that the rate-determining step of corrosion, i.e., active complex formation, is more associated than dissociated, which leads to a decrease in disorder.

Adsorption isotherm. The process of adsorption is the desorption of water molecules by adsorbing inhibitor molecules on the metal surface, and this process can also be described as an exchange process. From this we can see that the inhibitor is adsorbed on the metal surface and covers the surface (th) as the inhibitor concentration increases, the surface is covered to a higher degree and the efficiency increases. θ is a quantity indicating the effectiveness of the inhibitor and is taken as 100. Several types of isotherms have been used to describe this process. Freundlich adsorption isotherms were obtained, which can be expressed as follows:

$$\theta = K_{ads}C^n \qquad (3.2)$$

or

$$log\theta = logK_{ads} + nlogC \qquad (3.3)$$

where 0<n<1; θ– surface coating; C– inhibitor concentration; K_{ads}-equilibrium constant of the adsorption-desorption process.

The following isotherms for adsorption of these corrosion inhibitors were also studied

Lengmyur: $$\frac{C_{\mathrm{ing}}}{\theta} = \frac{1}{K_{ads}} + C_{\mathrm{ing}} \qquad (3.4)$$

Frumkin: $$\frac{\theta_{grav}}{1-\theta_{grav}} exp(-2f\theta_{grav}) = K_{ads}C_{ing} \qquad (3.5)$$

Tyomkin: $$exp(f\theta_{grav}) = K_{ads}C_{ing} \qquad (3.6)$$

where: C_{ing} - concentration of the inhibitor in the solution (mg/l),

θ- the full coverage rate,

K_{ads}- adsorption equilibrium constant.

The Langmuir isotherm provides a more complete understanding of the mechanism of interaction between the metal surface and the inhibitor. Using the Langmuir isotherm with C_{ing} bilan C_{ing}/θ as the adsorption equilibrium constant K_{ads} found by ΔG^0_{ads}value in the temperature range 25 ºC - 55 ºC is found using Equation 3.7:

$$\Delta G^0_{ads} = -RTln(1000K_{адс}) \qquad (3.7)$$

The standard free energy of adsorption (DG°ads) is calculated by the following equation (3.8).

$$\Delta G^o_{ads} = \Delta H^o_{ads} - T\Delta S^o_{ads} \qquad (3.8)$$

Here, R is the universal gas constant, T is the absolute temperature in Kelvin, and g/l. k_{ads} is the density of water in g/l. The values of cads and $\Delta G°_{ads}$ are calculated using the above isotherm equations.

In this case, E_a values were found from the dependence of lgW on 1000/T in mediums without and with inhibitors.

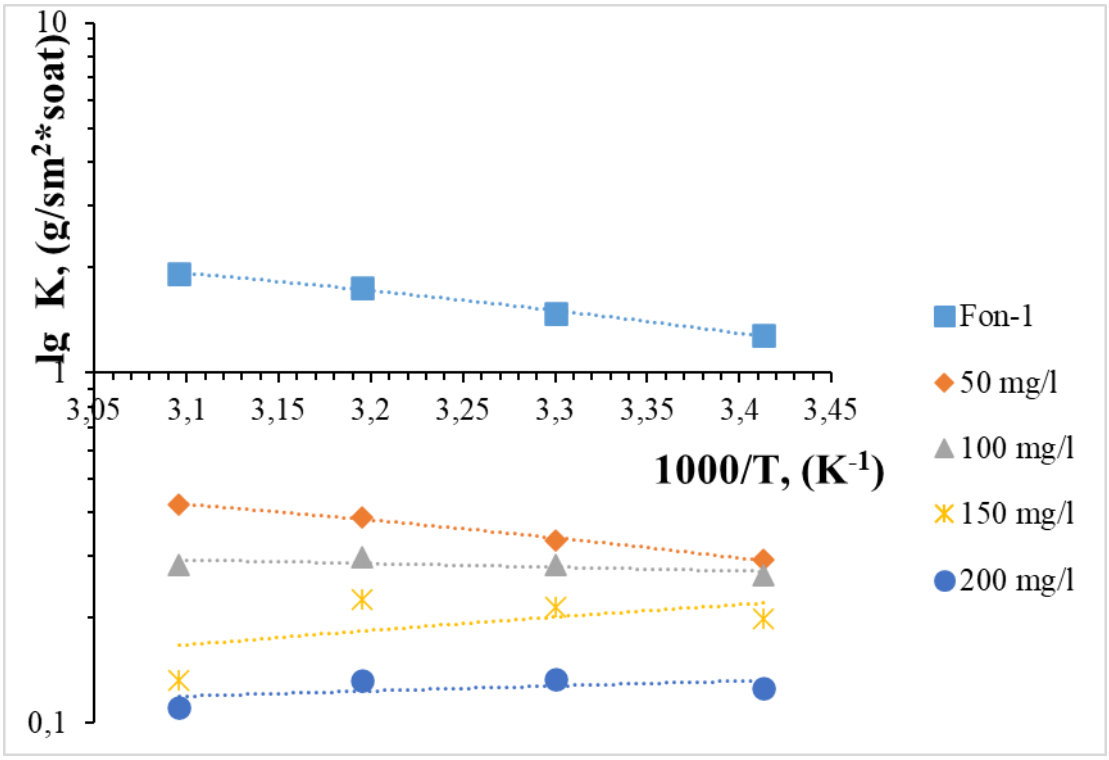

Figure 3.2. Arrhenius plot g for the activation energy of MMF-1 corrosion inhibitor in Fon-1 solution

According to the results presented in Table 3.13, the value of Ea was 41.45 (kJ/mol-1) in solutions without an inhibitor, this value increased with the introduction of MMF-1 brand corrosion inhibitor into the solution, and when the concentration reached 200 mg/l, it was 89.29 (kJ/mol-1). Also, the value of ΔSa in the solution without inhibitor took a positive value of 101.25 kJ/mol, but with the addition of inhibitor to the solution, this value decreased to negative -75.21 (kJ/mol-1), the smaller this value, the corrosion depends on the concentration of the inhibitor, the association is higher than dissociation in the system, and this indicates that a stable complex is formed between the inhibitor and the metal.

Table-3.4. Values of activation parameters for steel St20 in graded water without inhibitor and in presence of green inhibitor

Ingibitor konsentratsiyasi	E_a(kJ/mol^{-1})	ΔH_a (kJ/mol^{-1})	ΔS_a(kJ/mol^{-1}K^1)	$E_a - \Delta H_a$
0.0	41.45	38.4	101.25	2.94
50	53.26	51.43	-18.36	2.71
100	64.05	60.93	-23.12	2,64

150	76.30	72.62	-52.36	2.59
200	89.29	85.72	-75.21	2.47

The average energy difference between activation energy and enthalpy for samples without inhibitor and with different concentrations of inhibitor was approximately 2.67 kJ, which confirms the inhibition and adsorption process of St20 steel during melting.

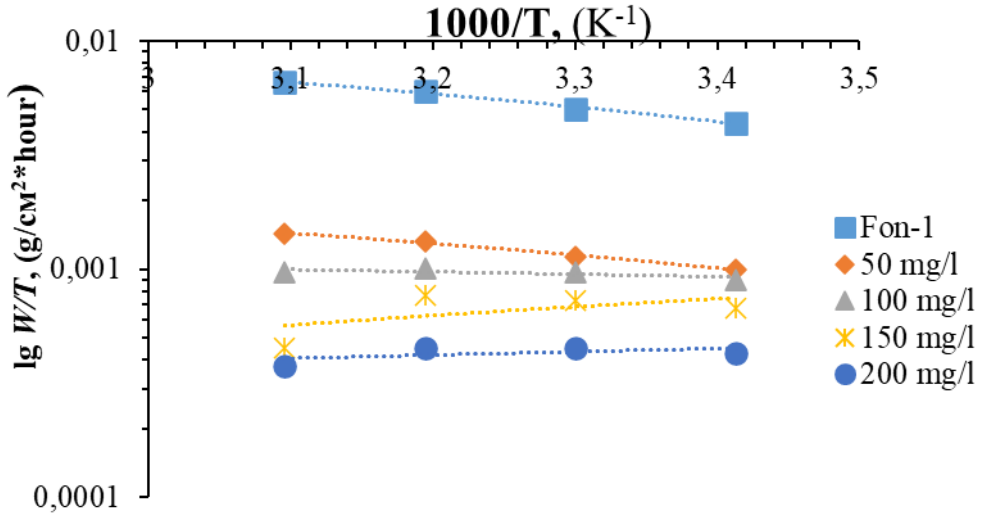

Figure 3.3. Transition state graph for the activation process of MMF-1 brand corrosion inhibitor in Fon-1 solution.

Several researchers have recognized that one of the reasons for the inhibition of the metal surface in the inhibitor solution is the absorption of the corrosion inhibitor on the surface. The presence of free ions in the composition of the corrosion inhibitor leads to the transport of charges, or the presence of functional groups binds to the metal surface through the donor-acceptor mechanism in exchange for negative charges. Langmuir, Frumkin, and Tyomkin isotherms of MMF-1 corrosion inhibitor were also studied.

Figure 3.4 of MMF-1 brand corrosion inhibitor. (a) Tyomkin (Figure 3.4 a), Frumkin (Figure 3.4 b), and Langmuir (Figure 3.4 c) isotherms are also plotted. According to the obtained results, when comparing the values of Frumkin, Tyomkin and Langmuir isotherms, the value of the Langmuir isotherm is higher than 0.99, which shows us that it matches the experimental data for the calculation of thermodynamic parameters. Langmuir, Frumkin, and Tyomkin isotherms for green corrosion inhibitors were also studied.

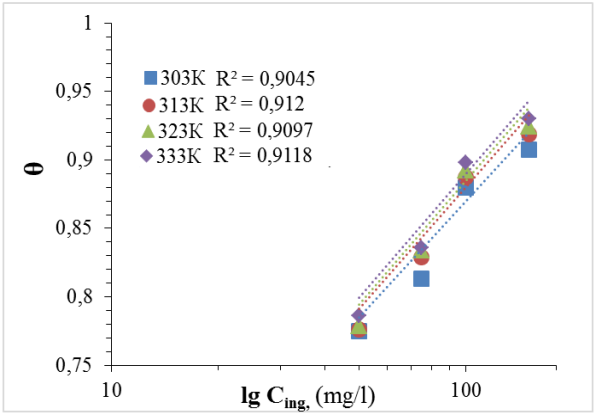

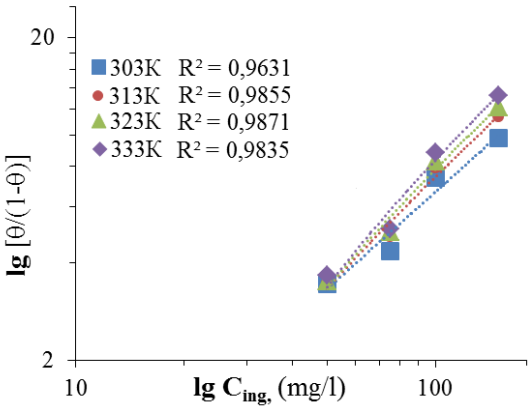

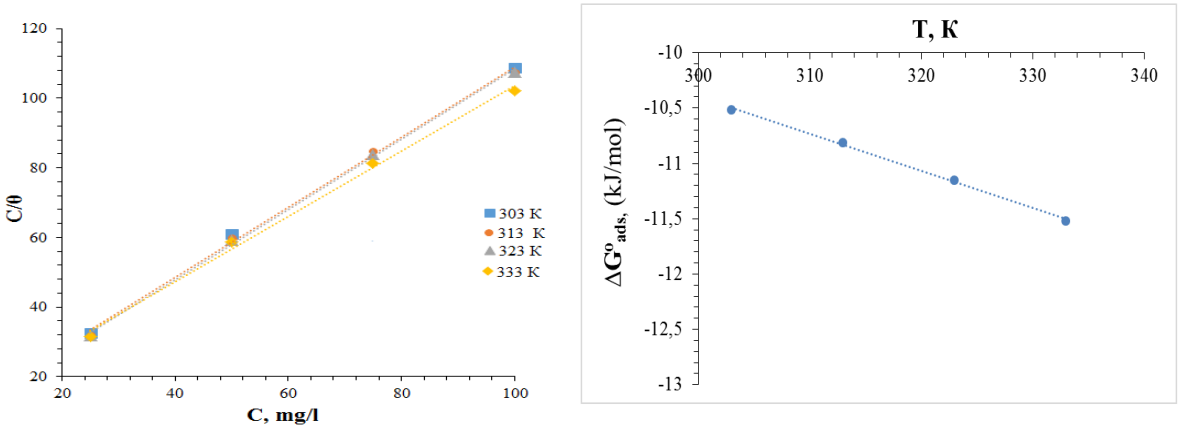

Figure 3.4. (a) Tyomkin, (b) Frumkin and (c) Langmuir isotherms and (d) temperature dependence of ΔG^0_{ads}

Correlation coefficient values were obtained at different temperatures. We can see from Figures 3.7a and 3.7b that the values of the correlation coefficients of the Frumkin and Tyomkin adsorption isotherms are not close to 1, indicating that the adsorption process does not follow these isotherms.

Table-3.5. Thermodynamic parameters of MMF-1 brand corrosion inhibitor

Temperature	K_{ads}	ΔG_{ads} kJ/mol	ΔH_{ads}, (kJ/mol)	ΔS_{ads}, (kJ/mol K)
303	356,7	-23,12	-15,38	-126,5
313	433,1	-25,23		
323	490,9	-26,25		
333	580,5	-28,29		

Then the values of K_{ads} were calculated based on the intersection of Langmuir isotherms. It follows from the values of $Kads$ that the adsorption of MMF-1 brand corrosion inhibitor on the metal surface is superior to all desorption. Judging from the data in Table 3.14, the values of ΔG0ads were obtained in the range of 303−333 K, with results ranging from negative -23.12 kJ/mol to-28.29 kJ/mol provided, thus confirming that the adsorption of MMF-1 brand corrosion inhibitor on the metal surface occurs spontaneously [17].

Scanning electron microscope analysis.

A scanning electron microscope (SEM) uses a focused beam of high-energy electrons on the surface of solid samples to produce a variety of signals. SEM allows obtaining information such as the surface structure (external morphology), chemical composition, orientation of components, as well as the crystal structure of the sample from the signals obtained from the electron interaction of the sample. The purpose of SEM analysis is to determine the presence of an inhibitor on the steel surface.

The pre-corrosion, post-corrosion and inhibited states of the steel surface were studied using a SEM-EVO MA 10 (Zeiss, Germany) scanning electron microscope.

Figure 3.5a. Original photograph of the steel sample

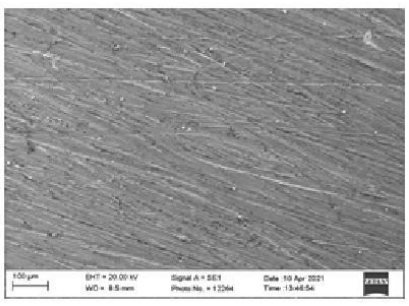

Figure 3.5b. SEM photograph of a steel sample

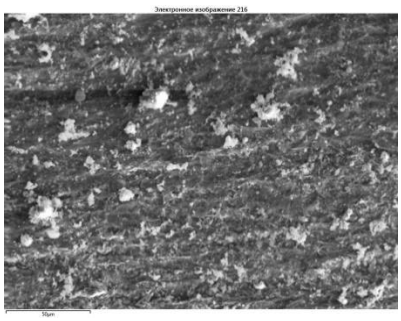

Figure 3.5c. SEM photograph of annealed steel sample

As you can see from the pictures given above, Figure 3.5a shows the first photo of a steel sample cleaned with different grades of sandpaper and washed in acetone. Also, microphotographs of the initial steel sample were taken using a scanning electron microscope in an environment without an inhibitor (Fig. 3.5b) and with an inhibitor (Fig. 3.5c).

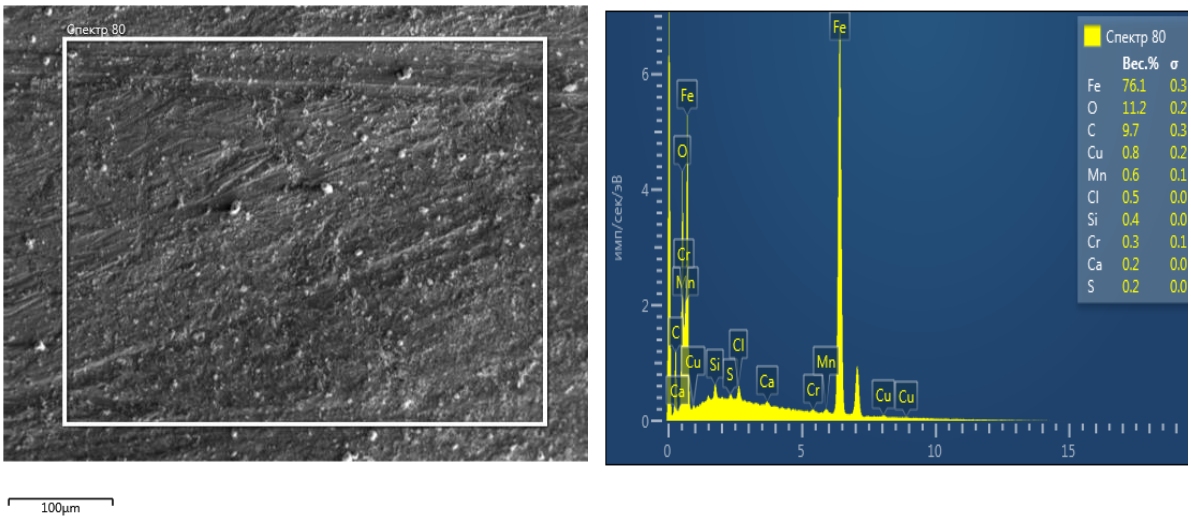

Figure 3.6. SEM and elemental analysis of St20 sample inhibited with MMF-1 inhibitor

It is known from Figure 3.6 that the SEM and elemental analysis of MMF-1 brand corrosion inhibitor in Fon-1 environment using a scanning electron microscope is presented. It is known that the inhibitor is adsorbed on the steel surface and protects against aggressive environments. It can also be seen from the element analysis.

4. Conclusion

It It is known from the results of the research that the optimal conditions for the synthesis of corrosion inhibitor based on maleic anhydride, monoethanolamine, and phosphoric acid were studied and its structure was analyzed using IR-spectra

The inhibition efficiency of the obtained corrosion inhibitor was studied based on gravimetric and electrochemical methods, and the results obtained by both types of methods completely repeated each other.

The inhibition mechanism of this inhibitor was studied based on Langmuir, Frumkin, and Tyomkin isotherms from the adsorption parameters and its effect on the steel surface using a scanning electron microscope.

References:

1. Verma, C.; Ebenso, E.; Bahadur, I.; Quraishi, M.: An overview on plant extracts as environmental sustainable and green corrosion inhibitors for metals and alloys in aggressive corrosive media. *J. Mol. Liq.* 2018, **266**, 577–590.
2. Umoren, S.; Solomon, M.; Obot, I.; Suleiman, R.: A critical review on the recent studies on plant biomaterials as corrosion inhibitors for industrial metals. *J. Indust. Eng. Chem*. 2019, **76**, 91–115.
3. Chigondo, M.; Chigondo, F.: Recent natural corrosion inhibitors for carbon steel : *an overview. J. Chem*. 2016. https://doi.org/10.1155/2016/6208937
4. Muthukrishnan, P.; Jeyaprabha, B.; Prakash, P.: Carbon steel corrosion inhibition by aqueous extract of Hyptis Suaveolens leaves. *Int. J. Ind. Chem*. 2014. https://doi.org/10.1007/s40090-014-0005-9.
5. Kaur, J., Daksh, N. & Saxena, A. Corrosion Inhibition Applications of Natural and Eco-Friendly Corrosion Inhibitors on Steel in the Acidic Environment: An Overview. *Arab J Sci Eng.* 2022, **47**, 57–74. https://doi.org/10.1007/s13369-021-05699-0.
6. Kouache A, Khelifa A, Boutoumi H, Moulay S, Feghoul A, Idir B, Aoudj S. Experimental and theoretical studies of Inula viscosa extract as a novel eco-friendly corrosion inhibitor for carbon steel in 1 M HCl. J *Adhes Sci Technol*. 2021, https://doi.org/10.1080/01694243.2021.195621
7. Lu, G., Li, YM., Lu, CH. *et al.* Corrosion protection of iron surface modified by poly(methyl methacrylate) using surface-initiated atom transfer radical polymerization (SI-ATRP). *Colloid Polym Sci.* 2010, **288**, 1445–1455. https://doi.org/10.1007/s00396-010-2283-x.
8. Nurilloev Z., Beknazarov Kh., Nomozov A. Production of corrosion inhibitors based on crotonaldehyde and their inhibitory properties. *International Journal of Engineering Trends and Technology*. 2021, **70**, 423-434. https://doi.org/10.14445/22315381/IJETT-V70I8P243.
9. Fariborz Atabaki, Jahangiri, S. & Pahnavar, Z. Thermodynamic and Electrochemical Investigations of Poly(Methyl Methacrylate–Maleic Anhydride) as Corrosion Inhibitors for Carbon steel in 0.5 M HCl. *Prot Met Phys Chem Surf.* 2019, **55**, 1161–1172. https://doi.org/10.1134/S2070205119060030.
10. Beknazarov, K. S., Dzhlilov, A. T., Ostanov, U. Y., & Erkaev A.M, "The Inhibition of the Corrosion of Carbon Steel by Oligomeric Corrosion Inhibitors in Different Media," *Int. Polym. Sci. Technol*, vol. 42, no. 4, pp. 33-37. Doi:10.1177/0307174x1504200406.

11. Kumar, S. Eco-friendly corrosion inhibitors: Synergistic effect of ethanol extracts of calotropis for corrosion of carbon steel in acid media using mass loss and thermometric technique at different temperatures. *Prot Met Phys Chem Surf*. 2016, **52**, 376–380. https://doi.org/10.1134/S2070205116020167
12. Baldin, EKK, Kunst, SR, Beltrami, LVR, Lemos, TM, Quevedo, MC, Bastos, AC, Ferreira, MGS, Santos, PRR, Sarmento, VHV, et al. "Ammonium Molybdate Added in Hybrid Films Applied on Tinplate Effect of the Concentration in the Corrosion Inhibition Action." *Thin Solid Films.* 2016, **600** 146–156.
13. Mouanga, M, Andreatta, F, Druart, ME, Marin, E, Fedrizzi, L, Olivier, MG, "A Localized Approach to Study the Effect of Cerium Salts as Cathodic Inhibitor on Iron/Aluminum Galvanic Coupling." *Corros. Sci.* 2015, **90** 491–502.
14. Rezaee, N, Attar, MM, Ramezanzadeh, B, "Studying Corrosion Performance, Microstructure and Adhesion Properties of a Room Temperature Zinc Phosphate Conversion Coating Containing Mn^{2+} on Carbon steel ." *Surf. Coat. Technol.*2013, **236** 361–367.
15. Muster, TH, Sullivan, H, Lau, D, Alexander, DLJ, Sherman, N, Garcia, SJ, Harvey, TG, Markley, TA, Hughes, AE, et al. "A Combinatorial Matrix of Rare Earth Chloride Mixtures as Corrosion Inhibitors of AA2024-T3: Optimisation Using Potentiodynamic Polarisation and EIS." *Electrochim. Acta*. 2012, **67** 95–103.
16. Nomozov A.K et all. Studying of Properties of Bitumen Modified based on Secondary Polymer Wastes Containing Zinc. International Journal of Engineering Trends and Technology. ISSN: 2231–5381 / https://doi.org/10.14445/22315381/IJETT-V71I9P222.
17. Nomozov A.K et all. Study of processe of obtaining monopotassium phosphate based on monosodium phosphate and potassium chloride. Chemical Problems. 2023 no. 3 (21). DOI: 10.32737/2221-8688-2023-3-279-293.